Journal of the Optical Society of America B
OPTICAL PHYSICS

Experimental measurement and analytical estimation of the signal gain in an Er-doped fiber

O. V. Shtyrina,[1,2] A. V. Ivanenko,[1,3] I. A. Yarutkina,[1,2] A. V. Kemmer,[1,3] A. S. Skidin,[1,2,*] S. M. Kobtsev,[1,3] and M. P. Fedoruk[1,2]

[1]Novosibirsk State University, 2 Pirogova Street, Novosibirsk 630090, Russia
[2]Institute of Computational Technologies, Siberian Branch of the Russian Academy of Sciences, 6 Ac. Lavrentjev Avenue, Novosibirsk 630090, Russia
[3]Tekhnoscan-Lab Ltd., 23 Inzhenernaya Street, Novosibirsk 630090, Russia
*Corresponding author: ask@skidin.org

Received 19 September 2016; revised 5 December 2016; accepted 6 December 2016; posted 6 December 2016 (Doc. ID 274768); published 4 January 2017

We propose a theoretical method to estimate the saturation power and the small signal gain of an active Er-doped fiber as functions of the fiber length and the pump power. The results make it possible to carry out the numerical simulation of a given Er-doped fiber. The results allow us to carry out the optimization of fiber laser systems by means of a numerical simulation using the nonlinear Schrödinger equation.

OCIS codes: (140.3500) Lasers, erbium; (140.3460) Lasers; (140.3430) Laser theory.

https://doi.org/10.1364/JOSAB.34.000227

1. INTRODUCTION

Nowadays, there is a wide range of fiber lasers of different cavity types [1]. Their internal structure may vary depending on the aim the laser is intended to achieve. To obtain stable generation in such lasers, it is necessary to compensate for the cavity losses. This can be achieved particularly by the use of an active medium. Currently the most common types of active fibers used in fiber lasers are erbium- (Er-) and ytterbium- (Yb)-doped fibers. Since Er^{3+}-doped fibers generate signals in the C-band (1.55 μm), they are widely employed in laser and amplification schemes that find their applications in many industrial areas. The main advantage of such fibers is that they allow one to minimize the losses in the fiber. Additionally, Er-doped fibers are widely applied in lasers to generate ultrashort pulses.

The Er-doped fiber signal gain can be analytically described using the two-level gain model [2]. The two-level model can be applied directly using the previously obtained analytical results [3]. The major drawback of the two-level model is that it does not take into account the background losses. Although the background losses are normally neglected for short cavities (with lengths up to several tens of meters), the consideration of the background losses improves the accuracy of numerical simulations. Furthermore, in many cases, it is necessary to take the background losses into consideration because they can be up to 70 dB/km [4].

Alternatively, the signal gain can be found numerically using a simple gain model that is based on the Schrödinger equation. Unlike the two-level model, the simple model takes into account the background losses. In order to be applied, it requires the signal gain to be bounded. This requirement, however, is always met, because usually, the signal gain is bounded above by the small signal gain [2]. In contrast with the two-level model, in the simple gain model, the saturation power and the small signal gain are functions of the pump power and the fiber length. In pulsed fiber lasers, the propagation of a signal in an active fiber is governed by the generalized nonlinear Schrödinger equation [5–21]:

$$\frac{\partial A}{\partial z} = -i\frac{\beta_2}{2}\frac{\partial^2 A}{\partial t^2} + \frac{\beta_3}{6}\frac{\partial^3 A}{\partial t^3} + i\gamma|A|^2 A + \frac{\hat{g}}{2}A - \frac{\alpha_A}{2}A, \quad (1)$$

where $A(t, z)$ is the complex envelope of the radiation, β_2 is the second-order dispersion, β_3 is the third-order dispersion, γ is the nonlinear parameter, and α_A denotes the background losses. When simulating the pulse propagation in the active fiber, the gain saturation is typically introduced into the frequency domain in the operator $\hat{g}$ as follows:

$$g(\omega) = \frac{1}{1 + P/P_{\text{sat}}} \times \frac{g_A}{1 + \left(\frac{\omega-\omega_0}{\Omega_g}\right)^2}. \quad (2)$$

Here, ω_0 is the central frequency of the gain, Ω_g is the gain bandwidth, g_A is the small signal gain, and P_{sat} is the saturation power. The gain is saturated with the growth of the average pulse power $P = \int |A|^2 \mathrm{d}t / T_R$, where T_R is the round-trip time.

In order to find the small signal gain g_A and the saturation power P_{sat}, we use the flat gain spectrum, since the input signal in the experiments is the CW pulse, so

$$\hat{g} = \frac{g_A}{1 + P/P_{\text{sat}}}. \quad (3)$$

It should be noted that to apply Eqs. (1) and (3), it is necessary to know the saturation power P_{sat} and the small signal gain g_A. They can be derived theoretically from the gain coefficients measured experimentally for various input powers, pump powers, and active fiber lengths. The increase of an Er-doped fiber length and the high pump power result in a large signal gain. Such a signal is seriously affected by the amplified spontaneous emission (ASE), and this makes it more difficult to measure the small signal gain. However, we need to know it in order to carry out the numerical simulation of the pulse propagation in Er fibers of various lengths. At the same time, the only way to obtain the small signal gain is to derive it analytically from other parameters, since most technical specifications of Er-doped fibers specify only the absorption coefficient at the pump wavelengths. This coefficient only allows us to estimate the optimal fiber length from the point of the pump absorption.

In this work, we present an experimental scheme for measuring the Er-doped fiber gain. During the experimental measurement of the signal gain in an Er-doped fiber, the dependence between the gain coefficient and the input signal power has been obtained for different fiber lengths and pump powers. In this paper, we also propose an algorithm for finding the parameters of Eq. (1) P_{sat}, and g_A, which are necessary to carry out the numerical simulation. The presented algorithm allows us to estimate the saturation power and the gain coefficient of Er-doped fibers of different lengths with different pump powers without needing to carry out additional experimental measurements.

2. EXPERIMENTAL SETUP

The measurement scheme of the Er fiber gain is shown in Fig. 1. It consists of an Er-doped fiber, a CW laser source, a variable attenuator, a multiplexer, a pump diode, and a spectrometer. The gain medium is of length 2.5 m, and its absorption coefficient is 30 dB/m.

The pump of the Er fiber is produced by a laser diode at 980 nm. Before the pump signal reaches the Er fiber, it passes through the multiplexer. The maximum pump power is 400 mW. To generate the input signal, continuous radiation of 15 mW generated by a CW laser at 1550 nm is used. Its spectrum is shown in Fig. 2. The output spectrum is registered using the spectrum analyzer with a resolution of 0.02 nm. To record both the input signal P_{in} and the output signal P_{out} simultaneously, an optical switch is used (Fig. 3). The switch connects the signal channels P_{in} and P_{out} to the spectrum analyzer, as shown in Fig. 3.

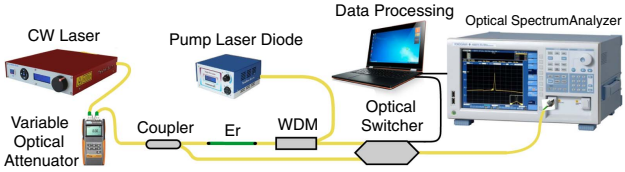

Fig. 1. Scheme of the experiment.

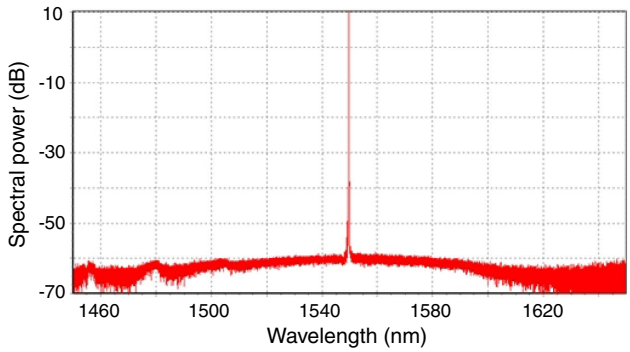

Fig. 2. Optical spectrum of the CW laser.

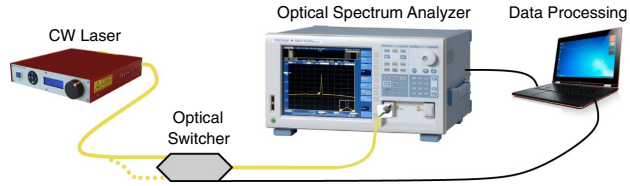

Fig. 3. Connection scheme of the spectrum analyzer.

The input power is varied using the variable attenuator. Its minimum attenuation is about 3 dB, and the maximum attenuation is 30 dB. Thus, the input signal power ranges from 7.5 mW to 15 μW. If the input signal power is less than 15 μW, it is difficult to register it because of the high noise of the spectrum analyzer. To overcome this limitation, couplers with high output coefficients (99%) are employed. Figure 4 shows the schemes to measure the signal gain.

Let us consider the measurement schemes shown in Fig. 4. The output pins of coupler 1 that carry 1% and 99% of the input power are denoted by CS1 and CL1, respectively. Similarly, we denote the same pins of coupler 2 by CS2 and CL2. Each scheme depicted in Fig. 4 covers the specific range of P_{in} values. Scheme 4a uses two couplers to make the input energy P_{in} as small as possible because it includes the second coupler. Once they are connected to each other, two couplers can reduce the input signal about 10,000 times. In this case, P_{in} is varied from 1.5 to 750 nW. The input energy for scheme 4b is between 150 nW and 75 μW. Scheme 4c gives the input power from 14.8 μW to 7.42 mW; these large values allow us to measure the saturation gain of the Er fiber. Taken together, schemes 4a, 4b, and 4c cover all possible values of the input energy P_{in} that might be of practical interest.

In Figs. 4(a) and 4(b), the output CL1 is connected to the spectral analyzer via the optical switch. This provides a reliable way to measure the input signal with a large signal-to-noise ratio.

Using the proposed schemes, it is possible to tune the power of the input radiation that enters the Er-doped fiber from 1.5 nW to 7.42 mW. When estimating the gain coefficient, the ASE noise power and the noise power of the spectral analyzer have been taken into account. In order to estimate the ASE power, the optical spectrum of the spectral analyzer, the optical

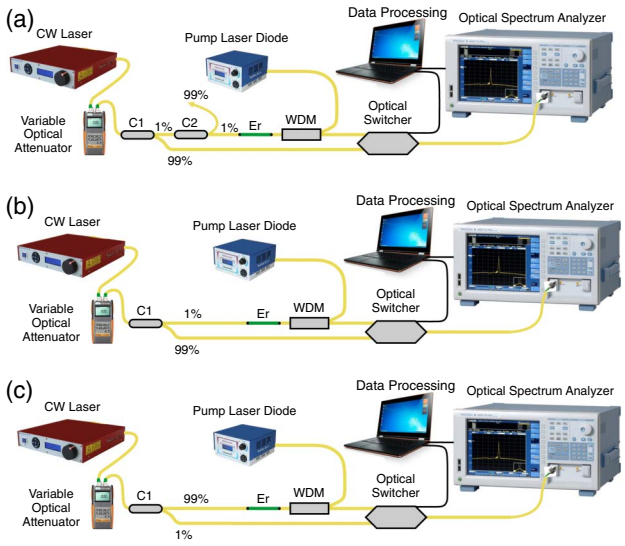

Fig. 4. Measurement schemes of the signal gain for different methods of the connection of two couplers 99/1.

spectrum of ASE for various pump powers, and the optical spectrum of a combined signal have been measured. The combined signal includes both the ASE and the input laser radiation. To improve the accuracy, the results obtained were averaged over 5 runs.

The relation between the output power and the input power has been estimated using the following formula:

$$\frac{P_{\text{out}}}{P_{\text{in}}} = \frac{P_{\text{out+ASE}} - P_{\text{ASE}} - P_{\text{noise}}}{P_{\text{laser}} \cdot \alpha - P_{\text{noise}}}. \tag{4}$$

Here, $P_{\text{out+ASE}}$ is the amplified signal power, P_{ASE} is the power of the ASE, P_{noise} is the noise power, P_{laser} is the input signal power, and α is the power transfer coefficient that depends on the scheme selected.

Using the described schemes, the experimental dependence of the gain coefficient on the input power has been obtained for different fiber lengths and different pump powers. Let us theoretically derive the dependence of the small signal gain and the saturation power on the pump power and the fiber length.

3. THEORETICAL APPROXIMATION

It can be shown [1] that the average power evolution in an active fiber can be described as follows:

$$\frac{\partial P}{\partial z} = P \times \left(\frac{g_A}{1 + P/P_{\text{sat}}} - \alpha_A \right), \tag{5}$$

where P denotes the average power, z is the spatial variable, t is the time variable, P_{sat} is the saturation power, α_A are the background losses, g_A is the small signal gain, L_A is the active fiber length.

Let us define P_{in} as the input power, and $P_{\text{out}} = P_{\text{in}} G$ as the power at the output of the active fiber. Here, G is the signal gain.

From Eq. (5), we can obtain [18,22]

$$P_{\text{in}} = \frac{1-s}{s} \times P_{\text{sat}} \times \frac{1 - G^s \exp[s(s-1)(g_A L_A + \alpha_A L_A)]}{G - G^s \exp[s(s-1)(g_A L_A + \alpha_A L_A)]}, \tag{6}$$

where $s = \alpha_A / g_A$.

Equation (6) allows us to find the output power P_{out} in a general case; however, in order to be applied correctly, it requires knowledge of the parameters P_{sat}, α_A, and g_A. We show below that these parameters can be derived from the experimental results. To find them, we propose an algorithm based on the theoretical analysis of the experimental results. Let us examine the algorithm in detail.

1. As a result of the experiment, we have the dependence of the signal gain G on the input power P_{in}. Signal gain G is measured for different lengths of the active fiber and for different pump powers. Thus, we denote G as a function of the pump power P_{pump}, active fiber length L_A, and the input power: $G = G(P_{\text{pump}}, L_A, P_{\text{in}})$. Similarly, the saturation power $P_{\text{sat}} = P_{\text{sat}}(P_{\text{pump}}, L_A)$, and the small signal gain $g_A = g_A(P_{\text{pump}}, L_A)$. At the same time, the coefficient α_A of the background losses remains constant for each measurement [4].

2. To estimate α_A, let us consider the limiting case of $P_{\text{in}} \to \infty$. Then, Eq. (5) can be rewritten as follows: $\frac{dP}{dz} = -\alpha_A P$. The solution of the equation is $P_{\text{out}} = P_{\text{in}} \cdot \exp(-\alpha_A L_A)$.

In order to find the background losses α_A, we consider the case of absorption, since in this case, the signal gain varies slowly with the change of the input signal power P_{in}.

The experimental results obtained with the following parameters are analyzed: $G = G(P_{\text{pump}} = 0\ \text{mW}, L_A = 0.52\ \text{m}, P_{\text{in}})$. The experimental results are depicted by the yellow dots in Fig. 5.

Using the method of least squares, the limiting value $G \to 0.677$ has been found. Then, $\alpha_A = -\ln(0.677)/L_A = 0.75$ [dB/m]. The method to find the rest of necessary values is presented below. As the result, the theoretical dependence of the gain G on P_{in} has been found. It is shown by the black line in Fig. 5.

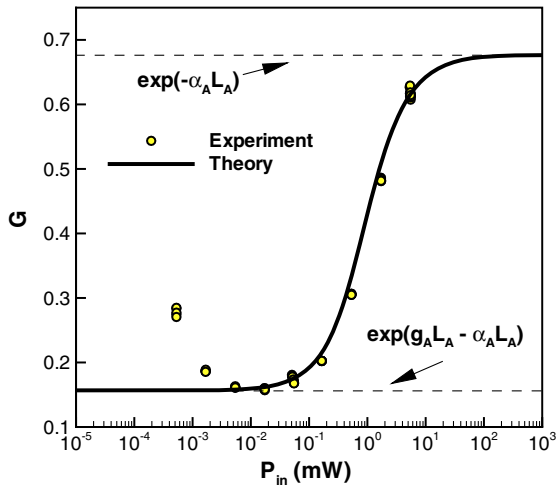

Fig. 5. Dependence of the gain coefficient on the input power; the pump power equals 0 mW (this corresponds to the case of absorption) and $\alpha_A = 0.75$ [dB/m].

Table 1. Gain Coefficient G Measured Experimentally for Different Active Fiber Lengths and Pump Powers in the Case of Small P_{in}

P_{pump}	$L_A = 0.52$ m	$L_A = 1.08$ m	$L_A = 2.0$ m	$L_A = 2.5$ m
31.2 mW	4.43	20	93	135
42.3 mW	4.84	28	214	331
61.4 mW	5.5	43.6	331	741
151 mW	7.16	60.25	891	—
198 mW	7.08	74	1096	—

3. Let us consider the case of $P_{in} \to 0$. Then, Eq. (5) can be transformed into the following: $\frac{dP}{dz} = (g_A - \alpha_A)P$. The solution of the equation is $P_{out} = P_{in} \cdot \exp(g_A L_A - \alpha_A L_A)$. In Fig. 5, the limit $P_{in} \to 0$ corresponds to the lower dashed line (in this case, $G = 0.156$, and $g_A = -2.8$ dB/m).

From the experiment, we have the values $G = G(P_{pump}, L_A, P_{in})$ for $L_A = 0.52$ m, 1.08, 2.0, and 2.5 m, and for $P_{pump} = 31.2$ mW, 42.3, 61.4, 151, and 198 mW.

We consider the experimental results for the fixed fiber length and pump power. For each experiment, we define the small signal gain using the signal gain G in the case of a small input signal power (Table 1) as follows: $g_A L_A = \ln G + \alpha_A L_A$ (Table 2).

4. For each set of experimental results for a given L_A and P_{pump}, the small signal gain and background losses are defined above; consequently, one can determine the saturation power as a function of the input signal power $P_{sat} = \hat{P}_{sat}(P_{in}, G)$ at each point of the experimental curve:

$$\hat{P}_{sat} = \frac{s}{1-s} \times P_{in} \times \frac{G - G^s \exp[s(s-1)(g_A L_A + \alpha_A L_A)]}{1 - G^s \exp[s(s-1)(g_A L_A + \alpha_A L_A)]}, \tag{7}$$

Using the root-mean-square method and Eq. (7), one can obtain the average saturation power for each experimental curve:

$$P_{sat} = \frac{\sum_{P_{in,i}} \hat{P}_{sat}(P_{in,i}, G_i)}{\sum_{P_{in,i}} 1}, \tag{8}$$

where $\sum_{P_{in,i}} 1$ is the number of points on the experimental curve, and $\hat{P}_{sat}(P_{in,i}, G_i)$ denotes the saturation power at the i-th point of the experimental curve that corresponds to a given pump power P_{pump} and given fiber length L_A. It is calculated via Eq. (7).

Using the proposed algorithm, one can find the theoretical dependence of G on P_{in} for each curve using P_{sat} obtained above and the implicit Eq. (6). Figure 6 shows the comparison of the experimental and theoretical results produced by the proposed algorithm. In Fig. 6, the colored dots illustrate the experimental results, and the solid curves illustrate the corresponding theoretical dependencies of G on P_{in} for different active fiber lengths and pump powers.

Table 2. Small Signal Gain g_A [dB/m] for Different Active Fiber Lengths and Pump Powers

P_{pump}	$L_A = 0.52$ m	$L_A = 1.08$ m	$L_A = 2.0$ m	$L_A = 2.5$ m
31.2 mW	3.6	3.52	3.01	2.71
42.3 mW	3.78	3.83	3.43	3.07
61.4 mW	4.02	4.24	3.65	3.39
151 mW	4.54	4.53	4.14	—
198 mW	4.5	4.73	4.25	—

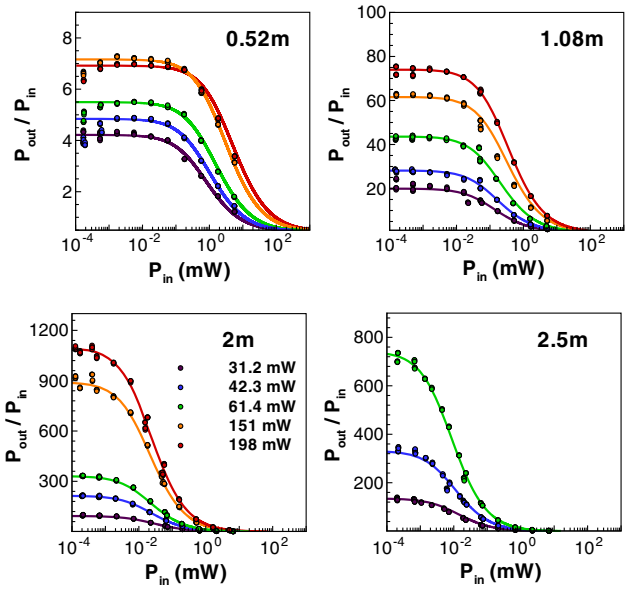

Fig. 6. Dependence of the gain coefficient on the input signal power for different fiber lengths and different pump powers. Here, the solid lines show the theoretical results, and the corresponding dots illustrate the experimental results.

It should be noted that the main reason for the difference between the experimental and numerical data at low powers in Fig. 5 is because of the error of the output and input power measurements and because of the error of the input power measurement in Fig. 6 in the case of $L_A = 0.52$ m. From Figs. 5 and 6, this error is about 10^{-3} mW. In Fig. 6, when the Er-doped fiber length grows, the measurement error becomes smaller compared to the output power. It is noteworthy to say that the error in the gain measurement in case of unsaturated gain does not affect the accuracy of the theory proposed in the paper for laser applications, because the theory is mainly intended to be applied to the practically realized cases of a saturated gain and significant input power.

The optimization of fiber laser systems requires a number of calculations for various fiber lengths and pump powers. To simplify a multiparametric optimization, we present the approximation that allows us to find the dependence of the saturation power and the small signal gain on the active fiber length and pump power without carrying out additional experimental measurements.

Figure 7(a) demonstrates the dependence between the saturation power P_{sat} and the pump power. The yellow dots correspond to the theoretical approximation of P_{sat} for various parameters. From Fig. 7(a), we can see that the saturation power depends linearly on the pump power and does not depend on the active fiber length. The dashed line in Fig. 7(a) corresponds to the following linear fitting formula:

$$P_{sat}[\text{mW}] = 0.1292 \cdot P_{pump}[\text{mW}] - 1.096[\text{mW}]. \tag{9}$$

The dependence of the small signal gain on the fiber length and pump power is shown in Fig. 7(b). It can be seen from

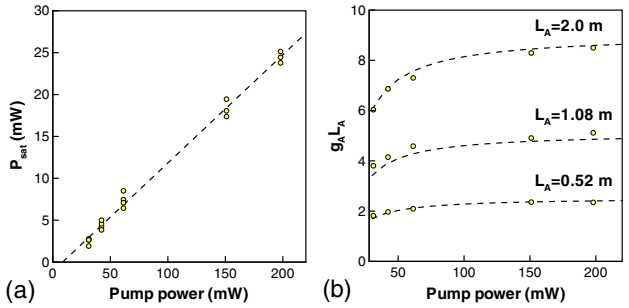

Fig. 7. (a) The dependence of the saturation power on the pump power for different fiber lengths. The dashed line demonstrates the linear fit. The yellow dots correspond to the theoretical approximation of P_{sat} for various parameters. (b) The dependence of $g_A L_A$ on the pump power for different fiber lengths. The yellow dots correspond to the theoretical approximation of $g_A L_A$ for various parameters. The dashed lines correspond to the theoretical dependence [Eq. (10)].

Fig. 7(b) that the small signal gain reaches the following limit for large pump powers:

$$g_A = \frac{A + B \cdot P_{\text{pump}}[\text{mW}]}{1 - C \cdot P_{\text{pump}}[\text{mW}] \exp(-DL_A)}. \quad (10)$$

Here, coefficients $A = -2.25 \cdot 10^5$ dB/m, $B = 2.3 \cdot 10^4$ dB/mW/m, $C = -4.54 \cdot 10^3$ l/mW, and $D = 0.05$ dB/m. The formula presented above was derived from the two-level effective gain model [4,23].

4. CONCLUSIONS

In this paper, the proposed measurement scheme enables us to measure the gain coefficient of an Er-doped fiber for input powers that are varied over a wide range. During the experiment, the dependence of the gain coefficient on the input power has been found for different fiber lengths and pump powers. The theoretical method to estimate the saturation power and the small signal gain coefficients of the Er-doped fiber has been proposed. The results may be useful for optimization of the fiber laser systems by means of a numerical simulation.

Funding. Ministry of Education and Science of the Russian Federation (Minobrnauka) (14.B25.31.0003, RFMEFI57814X0029); Russian Foundation for Basic Research (RFBR) (16-32-60160).

Acknowledgment. The authors are grateful to Sergey Smirnov for consultation during the experiment and Artur Golubtsov for assistance in the implementation of the experimental data collection system. The work of A. V. Kemmer and S. M. Kobtsev was supported by the Ministry of Education and Science of the Russian Federation. The work of A. V. Ivanenko was supported by the Russian Foundation for Basic Research. The work of A. S. Skidin was supported by the Ministry of Education and Science of the Russian Federation.

REFERENCES

1. A. E. Siegman, *Lasers* (University Science Books, 1986).
2. E. Desurvire, *Erbium-Doped Fiber Amplifiers: Principles and Applications* (1994).
3. T. Pfeiffer and H. Büllow, "Analytical gain equation for erbium-doped fiber amplifiers including mode field profiles and dopant distribution," IEEE Photon. Technol. Lett. **4**, 449–451 (1992).
4. C. Barnard, P. Myslinski, J. Chrostowski, and M. Kavehrad, "Analytical model for rare-earth-doped fiber amplifiers and lasers," IEEE J. Quantum Electron. **30**, 1817–1830 (1994).
5. H. A. Haus, "Theory of mode locking with a slow saturable absorber," IEEE J. Quantum Electron **11**, 736–746 (1975).
6. H. A. Haus, J. G. Fujimoto, and E. P. Ippen, "Analytic theory of additive pulse and Kerr lens mode locking," IEEE J. Quantum Electron. **28**, 2086–2096 (1992).
7. S. Namiki, E. P. Ippen, H. A. Haus, and C. X. Yu, "Energy rate equations for mode-locked lasers," J. Opt. Soc. Am. B **14**, 2099–2111 (1997).
8. J. N. Kutz, "Mode-locked soliton lasers," SIAM Rev. **48**, 629–678 (2006).
9. S. Smirnov, S. Kobtsev, S. Kukarin, and A. Ivanenko, "Three key regimes of single pulse generation per round trip of all-normal-dispersion fiber lasers mode-locked with nonlinear polarization rotation," Opt. Express **20**, 27447–27453 (2012).
10. A. V. Ivanenko, S. M. Kobtsev, S. V. Kukarin, and A. S. Kurkov, "Femtosecond Er laser system based on side-coupled fibers," Laser Phys. **20**, 341–343 (2010).
11. T. Schreiber, B. Ortaç, J. Limpert, and A. Tünnermann, "On the study of pulse evolution in ultra-short pulse mode-locked fiber lasers by numerical simulations," Opt. Express **15**, 8252–8262 (2007).
12. F. W. Wise, A. Chong, and W. H. Renninger, "High-energy femtosecond fiber lasers based on pulse propagation at normal dispersion," Laser Photon. Rev. **2**, 58–73 (2008).
13. V. L. Kalashnikov, E. Podivilov, A. Chernykh, and A. Apolonski, "Chirped-pulse oscillators: theory and experiment," Appl. Phys. B **83**, 503–510 (2006).
14. P. Grelu and N. Akhmediev, "Dissipative solitons for mode-locked lasers," Nat. Photonics **6**, 84–92 (2012).
15. X. Liu, "Numerical and experimental investigation of dissipative solitons in passively mode-locked fiber lasers with large net-normal-dispersion and high nonlinearity," Opt. Express **17**, 22401–22416 (2009).
16. A. Martinez and S. Yamashita, "Multi-gigahertz repetition rate passively modelocked fiber lasers using carbon nanotubes," Opt. Express **19**, 6155–6163 (2011).
17. O. Shtyrina, M. Fedoruk, S. Turitsyn, R. Herda, and O. Okhotnikov, "Evolution and stability of pulse regimes in SESAM-mode-locked femtosecond fiber lasers," J. Opt. Soc. Am. B **26**, 346–352 (2009).
18. S. K. Turitsyn, "Theory of energy evolution in laser resonators with saturated gain and non-saturated loss," Opt. Express **17**, 11898–11904 (2009).
19. B. G. Bale, S. Boscolo, J. N. Kutz, and S. K. Turitsyn, "Intracavity dynamics in high-power mode-locked fiber lasers," Phys. Rev. A **81**, 033828 (2010).
20. S. K. Turitsyn, B. Bale, and M. P. Fedoruk, "Dispersion-managed solitons in fibre systems and lasers," Phys. Rep. **521**, 135–203 (2012).
21. B. G. Bale, O. G. Okhotnikov, and S. K. Turitsyn, "Modeling and technologies of ultrafast fiber lasers," in *Fiber Lasers*, O. G. Okhotnikov, ed. (Wiley, 2012).
22. I. A. Yarutkina, O. V. Shtyrina, A. Skidin, and M. P. Fedoruk, "Theoretical study of energy evolution in ring cavity fiber lasers," Opt. Commun. **342**, 26–29 (2015).
23. S. K. Turitsyn, A. E. Bednyakova, M. P. Fedoruk, A. I. Latkin, A. A. Fotiadi, A. S. Kurkov, and E. Sholokhov, "Modeling of CW Yb-doped fiber lasers with highly nonlinear cavity dynamics," Opt. Express **19**, 8394–8405 (2011).